

Generation of squeezed states of magnons and photons based on the Kerr effect in cavity-magnon hybrid system

Cheng-Hua Bai(白成华) and Suying Bai(白素英)
Citation: Chin. Phys. B, 2026, 35 (**4**): 044210. DOI: 10.1088/1674-1056/ae4b2d
http://cpb.iphy.ac.cn; http://iopscience.iop.org/cpb

What follows is a list of articles you may be interested in

Effects of the buffer layer on the Casimir pressure of peptide films deposited on a substrate

Dingding Lv(吕丁丁), Shuai Zhou(周帅), Kaipeng Liu(柳开鹏), Shiwei Dai(戴士为), and Lixin Ge(葛力新)
Chin. Phys. B, 2025, 34 (**10**): 104202. DOI: 10.1088/1674-1056/adde36

Electromagnetically-induced-absorption-like ground state cooling in a hybrid optomechanical system

Yaoyong Dong(董耀勇), Xuejun Zheng(郑学军), Denglong Wang(王登龙), and Peng Zhao(赵鹏)
Chin. Phys. B, 2025, 34 (**4**): 044203. DOI: 10.1088/1674-1056/adb260

Quantum-state engineering using enhanced tripartite interactions in atom-photon-phonon hybrid systems

Yaowu Guo(郭耀武), Jiaqiang Zhao(赵加强), Lianzhen Cao(曹连振), Yingde Li(李英德), and Hong-Yan Lu(路红艳)
Chin. Phys. B, 2025, 34 (**2**): 024203. DOI: 10.1088/1674-1056/ad9a5d

Giant enhancement of negative friction by resonant coupling between localized surface phonon polaritons and graphene plasmonics

Kaipeng Liu(柳开鹏), Shuai Zhou(周帅), Shiwei Dai(戴士为), and Lixin Ge(葛力新)
Chin. Phys. B, 2025, 34 (**1**): 014202. DOI: 10.1088/1674-1056/ad886c

Phase sensitivity with a coherent beam and twin beams via intensity difference detection

Jun Liu(刘俊), Tao Shao(邵涛), Chenlu Li(李晨露), Minyang Zhang(张敏洋), Youyou Hu(胡友友), Dongxu Chen(陈东旭), and Dong Wei(卫栋)
Chin. Phys. B, 2024, 33 (**1**): 014203. DOI: 10.1088/1674-1056/ad0115

Generation of squeezed states of magnons and photons based on the Kerr effect in cavity-magnon hybrid system

Cheng-Hua Bai(白成华)[1,†] and Suying Bai(白素英)[2,‡]

[1] *School of Semiconductor and Physics, North University of China, Taiyuan* 030051, *China*
[2] *School of Physics and Information Engineering, Shanxi Normal University, Taiyuan* 030031, *China*

(Received 18 January 2026; revised manuscript received 19 February 2026; accepted manuscript online 27 February 2026)

Based on the magnon Kerr effect, we show how to generate quantum squeezed states of magnons and photons in the cavity–magnon hybrid system. We find that the squeezing of magnons can be successfully induced by the magnon nonlinearity and the larger two-magnon effect strength will be beneficial to achieving the stronger squeezing of magnon. Resorting to the beam-splitter interaction between the magnons and photons, we further show that the squeezing of photons can be also effectively achieved. By properly choosing the system parameters, we demonstrate that the desired direction of the generated squeezing both for magnons and photons can be flexibly switched between orthogonal directions. Our scheme provides an alternative manipulation method to explore the quantum phenomena with nonlinear effects and also has significant potential applications in quantum precision measurement.

Keywords: quantum squeezing, magnon Kerr effect, cavity–magnon hybrid system

PACS: 42.50.Lc, 42.50.Dv, 71.36.+c

DOI: 10.1088/1674-1056/ae4b2d **CSTR:** 32038.14.CPB.ae4b2d

1. Introduction

Cavity magnonics, the study of the interaction between microwave cavity and collective spin excitations (magnons) in magnetic materials, such as yttrium iron garnet (YIG), has made significant progress and also attracted extensive interest in recent years.[1–4] One of the most prominent advantages for the magnonic system is that it shows the excellent scalability via coherently coupling with other physical systems, such as microwave photons,[5,6] optical photons,[7,8] superconducting qubits,[9,10] vibration phonons,[11,12] and so on. Therefore, the magnonic system has been a highly potential candidate to build a desired hybrid system with multiple components, which accumulates the respective advantages of all subsystems and has wide applications in the fields of quantum information processing,[13] quantum network,[14] and quantum sensing.[15]

On the other hand, quantum fluctuations, the unique properties of quantum physics, produce some well-known interesting physical effects, such as Casimir forces and Lamb shift.[16] However, quantum fluctuations can also lead to some undesirable restrictions in precision measurements. For example, quantum fluctuations can broaden the optical response spectrum and influence the detection sensitivity inevitably.[17] Fortunately, quantum fluctuations are not immutable and can be effectively manipulated. It is well known that the quantum fluctuations of a pair of quadrature observations are dominated by the Heisenberg uncertainty principle.[18] Once the quantum fluctuation of either of the two quadratures is reduced below the standard quantum limit, it will lead to the corresponding increased fluctuation in the conjugate direction. This is the so-called quantum squeezed state. Therefore, squeezing of quantum fluctuation to achieve such a nonclassical quantum state plays an important role in the field of quantum-related technologies, such as sideband cooling beyond the quantum back-action limit[16] and quantum key distribution in microwave quantum communication.[19]

Meanwhile, the magnon system, in particular the YIG sphere with very high spin density ($\rho_s = 4.22 \times 10^{27}$ m^{-3}) and low damping rate,[6] provides a completely new platform to investigate the novel quantum phenomena and generate the various quantum states of magnons, such as Bell state,[20] W state,[21] NOON state,[22] non-Gaussian state,[23] and non-reciprocal microwave-optical entanglement.[24] To date, we note that only a few proposals have been proposed in cavity magnonics to generate magnon squeezed states. They can be realized by driving the cavity with squeezed vacuum field and further exploiting the cavity–magnon state-swap interaction,[25] driving the cavity with two-tone fields and further exploiting the phonon–magnon squeezing transfer,[26] directly driving the magnon mode with two-tone fields,[27] two-tone driving of a qubit coupled to the magnon mode.[28] Different from the above mentioned mechanisms, here we propose how to prepare magnon squeezed state based on the magnon Kerr effect in cavity–magnon hybrid system instead of using squeezed field driving or two-tone driving. We find that the magnon self-nonlinearity can successfully induce the

†Corresponding author. E-mail: chbai2021@foxmail.com
‡Corresponding author. E-mail: sybai2021@foxmail.com

© 2026 Chinese Physical Society and IOP Publishing Ltd. All rights, including for text and data mining, AI training, and similar technologies, are reserved.

magnon mode into steady squeezed state from the initial coherent state. The strong two-magnon effect strength helps to the generation of larger squeezing of magnon. We also demonstrate that the squeezing of cavity photon is simultaneously achieved by the cavity–magnon beam-splitter interaction. More importantly, in the proper regime of system parameter, the squeezing directions of the generated squeezed states both for magnon and photon can be flexibly controllable. Our scheme has promising applications in quantum precision measurement.

In addition, we note that Kani *et al.* also present a theoretical scheme for generating squeezed photons and magnons very recently.[29] In Ref. [29], the polarizations of the microwave and the external field are parallel and the mechanism is based on the nonlinear parametric coupling between magnon mode and cavity, i.e., $i\hbar g(as^{\dagger 2} - a^{\dagger}s^2)$. In their scheme, the system dynamics is characterized by the noise power spectral density $S(\omega)$ in the frequency domain. While in our scheme, the polarization of the microwave and the external field is vertical, and the magnon Kerr nonlinearity and linear photon–magnon coupling are exploited to achieve the squeezing of magnons and photons. More importantly, from the variance dynamics evolution and Wigner function in the phase space, we find that the direction of the generated squeezing both for magnons and photons is not fixed and can be switched flexibly between orthogonal directions.

Here we further compare the distinct differences between the present scheme and a prior work.[30] In Ref. [30], it is demonstrated that the bistability phenomena of squeezing and entanglement can be effectively achieved based on a nonlinear cavity magnonic system. Compared with this work, our scheme has the following distinct differences. (i) Although our work and Ref. [30] both resort to the magnon Kerr nonlinearity, the driving regime of microwave field in the system model is completely different. In Ref. [30], the magnon mode is directly driven by a microwave field, while the microwave cavity is driven by the microwave field in our work. (ii) The research results are completely different. In Ref. [30], it focuses mainly on the bistability of squeezing and entanglement in the experimentally feasible parameters, i.e., the quantum states can jump from one state to another state near the switching points. However, in our work, we mainly demonstrate that the desired direction of the generated squeezing both for magnons and photons can be flexibly switching between orthogonal directions in the experimentally feasible parameters. (iii) Besides the Wigner function in the phase space and decoherence factors (bath temperature and cavity dissipation) discussed in Ref. [30], our work also shows the discussion from variance dynamics, which clearly displays the oscillation behavior when the system does not reach its steady state yet.

The rest of this paper is organized as follows. In Section 2, we introduce the cavity–magnon hybrid system and provide the corresponding Hamiltonian. Then we derive the dynamical equation about the covariance matrix in Section 3. In Sections 4 and 5, we provide a detailed discussion on the generation of squeezing for magnon and photon, respectively. In Section 6, the experimental feasibility is briefly analyzed. Finally, we give a conclusion in Section 7.

2. Model and Hamiltonian

As shown in Fig. 1(a), we consider a cavity–magnon hybrid system, which consists of a strongly driven cavity with frequency ω_a and decay rate κ_a and a micron-size YIG sphere with frequency ω_m and decay rate γ_m, in which the YIG sphere is placed in a controllable magnetic field B_0. The Hamiltonian of this hybrid system is (setting $\hbar = 1$)

$$\begin{aligned} H \;=\; & \omega_a a^{\dagger}a + \omega_m m^{\dagger}m + g_m(a + a^{\dagger})(m + m^{\dagger}) \\ & + \Omega_0(a^{\dagger}\,\mathrm{e}^{-\mathrm{i}\omega_{\mathrm{L}}t} + a\,\mathrm{e}^{\mathrm{i}\omega_{\mathrm{L}}t}) + K_0(m^{\dagger}m)^2, \end{aligned} \tag{1}$$

where a and m ($a^{\dagger}$ and $m^{\dagger}$) are, respectively, the annihilation (creation) operators of the cavity and magnon modes. The tunable coupling coefficient g_m is the magnetic dipole coupling strength between the cavity and the Kittel mode, Ω_0 denotes the amplitude of the driving field, and K_0 is the Kerr nonlinearity of magnons in the Kittle mode. Experimentally, K_0 is reversely proportional to the size of the YIG sphere[31,32] and as shown in Fig. 1(b), the sign of K_0 can be controlled by changing the magnetic field B_0. So far, K_0 has been manipulated from 0.05 nHz to 100 nHz, corresponding to the size of the YIG sphere from 1 mm to 100 μm.[33] In the rotating frame with respect to the driving frequency ω_{L}, the Hamiltonian can be transformed to

$$\begin{aligned} H_1 \;=\; & \Delta_a a^{\dagger}a + \Delta_m m^{\dagger}m + g_m(am^{\dagger} + a^{\dagger}m) \\ & + \Omega_0(a^{\dagger} + a) + K_0(m^{\dagger}m)^2, \end{aligned} \tag{2}$$

where the detunings $\Delta_a = \omega_a - \omega_{\mathrm{L}}$ and $\Delta_m = \omega_m - \omega_{\mathrm{L}}$. In addition, in the parameter regime of $\omega_{\mathrm{L}} \gg g_m$, the high-frequency oscillating terms $\exp[\pm 2\mathrm{i}\omega_{\mathrm{L}}t]$ have been ignored via the rotating-wave approximation.

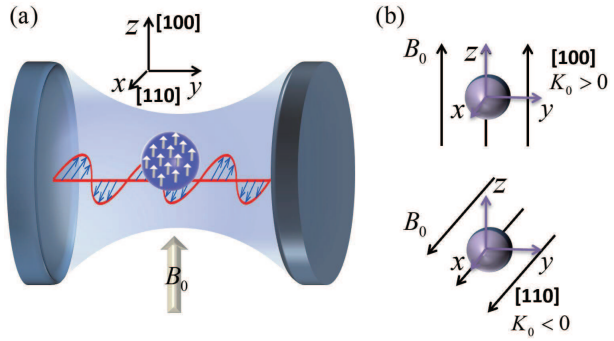


Fig. 1. (a) Schematic plot of the proposed cavity–magnon hybrid system. It is composed of a cavity pumped by the driving field with frequency ω_{L} and a YIG sphere with Kerr nonlinearity. Moreover, the YIG sphere is trapped in a controllable magnetic field with strength B_0 along the crystallographic axis [100] or [110]. (b) When the magnetic field B_0 is in the direction of crystallographic axis [100] or [110], the Kerr coefficient K_0 is positive or negative, respectively.

Taking the decay rates of the cavity and magnon modes into account, the quantum dynamics of the present hybrid system can be obtained with the Heisenberg–Langevin approach

$$\begin{aligned}\dot{a} &= \mathrm{i}[H_1,a]-\kappa_a a+\sqrt{2\kappa_a}a_{\rm in}\\ &= -(\mathrm{i}\Delta_a+\kappa_a)a-\mathrm{i}g_m m-\mathrm{i}\Omega_0+\sqrt{2\kappa_a}a_{\rm in},\\ \dot{m} &= \mathrm{i}[H_1,m]-\gamma_m m+\sqrt{2\gamma_m}m_{\rm in}\\ &= -(\mathrm{i}\Delta_m+\gamma_m)m-\mathrm{i}g_m a-2\mathrm{i}K_0 m^\dagger mm+\sqrt{2\gamma_m}m_{\rm in},\end{aligned}\tag{3}$$

where $a_{\rm in}$ and $m_{\rm in}$ are input noise operators corresponding to the cavity and magnon modes, respectively. They are zero mean and their correlation functions are[12,34] $\langle a_{\rm in}(t)a_{\rm in}^\dagger(t')\rangle=(N_a+1)\delta(t-t')$, $\langle a_{\rm in}^\dagger(t)a_{\rm in}(t')\rangle=N_a\delta(t-t')$, $\langle m_{\rm in}(t)m_{\rm in}^\dagger(t')\rangle=(N_m+1)\delta(t-t')$, and $\langle m_{\rm in}^\dagger(t)m_{\rm in}(t')\rangle=N_m\delta(t-t')$, where $N_o=\{\exp[(\hbar\omega_o/k_{\rm B}T)-1]\}^{-1}$ ($o=a$ and m) is the mean thermal excitation number in the cavity and magnon modes. Here $k_{\rm B}$ is the Boltzmann constant and T is the bath temperature. It should be pointed out that in a general nonlinear cavity magnonic system,[30,35] $K_0\sim\mu$Hz and $\Delta_m\sim$MHz. Under the condition of $\Delta_m\gg K_0$, the term $-\mathrm{i}K_0 m$ in Eq. (3) has been ignored safely. In the strong driving condition, the cavity and magnon modes will induce high amplitudes so that the standard linearization method can be applied into Eq. (3).[12,36–38] To this end, we expand cavity mode a and magnon mode m as the sum of the mean value and the quantum fluctuation operator, i.e., $O\to\langle O\rangle+\delta O$, with $O=a,m$. Therefore, by neglecting the high-order fluctuation terms, the linearized quantum Langevin equations for the quantum fluctuations are given by

$$\begin{aligned}\delta\dot{a} &= -(\mathrm{i}\Delta_a+\kappa_a)\delta a-\mathrm{i}g_m\delta m+\sqrt{2\kappa_a}a_{\rm in},\\ \delta\dot{m} &= -(\mathrm{i}\Delta_m'+\gamma_m)\delta m-\mathrm{i}g_m\delta a-\mathrm{i}K\delta m^\dagger+\sqrt{2\gamma_m}m_{\rm in},\end{aligned}\tag{4}$$

where $\Delta_m'=\Delta_m+\Delta_K$, with the magnon frequency detuning Δ_m and the magnon frequency shift $\Delta_K=2K$, is the effective magnon frequency detuning induced by the magnon Kerr effect. Here the defined parameter $K=2K_0\langle m\rangle^2$ describes the strength of the two-magnon effect. The linearized Hamiltonian of the present hybrid system is correspondingly obtained,

$$\begin{aligned}H_{\rm lin} &= \Delta_a\delta a^\dagger\delta a+\Delta_m'\delta m^\dagger\delta m+g_m(\delta a\delta m^\dagger+\delta m\delta a^\dagger)\\ &\quad+\frac{K}{2}(\delta m^2+\delta m^{\dagger 2}).\end{aligned}\tag{5}$$

Obviously, it can be seen that the above Hamiltonian takes the form of $\delta m^2+\delta m^{\dagger 2}$ that is induced by the Kerr effect and the corresponding evolution operator is a squeezed operator, so it is possible to create quadrature squeezing of the magnon mode[18,39] and the cavity field can be also prepared in a squeezed state via the cavity–magnon beam-splitter interaction $\delta a\delta m^\dagger+\delta m\delta a^\dagger$. On the other hand, it is evident that the frequency shift Δ_m' will influence the squeezed operator in the interaction picture. Hence, it leads to the squeezing of quadrature-dependent fluctuation. In the following, we will characterize the squeezing effect via the system dynamics.

3. System dynamics

For convenience, the following quadrature fluctuation operators are introduced:

$$\begin{aligned}\delta X_a &= (\delta a+\delta a^\dagger)/\sqrt{2},\ \ \delta Y_a=(\delta a-\delta a^\dagger)/(\sqrt{2}\mathrm{i}),\\ \delta X_m &= (\delta m+\delta m^\dagger)/\sqrt{2},\ \ \delta Y_m=(\delta m-\delta m^\dagger)/(\sqrt{2}\mathrm{i}),\end{aligned}\tag{6}$$

and the quadrature noise operators are

$$\begin{aligned}X_a^{\rm in} &= (a_{\rm in}+a_{\rm in}^\dagger)/\sqrt{2},\ \ Y_a^{\rm in}=(a_{\rm in}-a_{\rm in}^\dagger)/(\sqrt{2}\mathrm{i}),\\ X_m^{\rm in} &= (m_{\rm in}+m_{\rm in}^\dagger)/\sqrt{2},\ \ Y_m^{\rm in}=(m_{\rm in}-m_{\rm in}^\dagger)/(\sqrt{2}\mathrm{i}).\end{aligned}\tag{7}$$

Then the linearized system dynamics in Eq. (4) can be written in the following compact form:

$$\dot{R}(t)=MR(t)+N(t),\tag{8}$$

where $R(t)=[\delta X_a,\delta Y_a,\delta X_m,\delta Y_m]^{\rm T}$ and $N(t)=[\sqrt{2\kappa_a}X_a^{\rm in},\sqrt{2\kappa_a}Y_a^{\rm in},\sqrt{2\gamma_m}X_m^{\rm in},\sqrt{2\gamma_m}Y_m^{\rm in}]^{\rm T}$ are the column vectors for the quantum fluctuations and input noise, respectively. The 4×4 matrix M is

$$M=\begin{pmatrix}-\kappa_a & \Delta_a & 0 & g_m\\ -\Delta_a & -\kappa_a & -g_m & 0\\ 0 & g_m & -\gamma_m & \Delta_m'-K\\ -g_m & 0 & -(\Delta_m'+K) & -\gamma_m\end{pmatrix}.\tag{9}$$

Based on the Rough–Hurwitz criterion,[40] when all of the eigenvalues of matrix M have negative real parts, the system dynamics in the long-time limit is stable.

Generally, thanks to the linearized dynamics characteristic in Eq. (8) and the zero-mean Gaussian nature of the input quantum noises, it is extremely convenient to introduce the covariance matrix (CM) to describe the system dynamics.[41–43] To this end, we define the following 4×4 CM V:

$$V_{j,k}=\langle R_j(t)R_k(t)+R_k(t)R_j(t)\rangle/2,\ \ (j,k=1,2,3,4).\tag{10}$$

Combining Eqs. (8) and (10), we can derive the equation of motion about V

$$\dot{V}(t)=MV(t)+V(t)M^{\rm T}+D,\tag{11}$$

where $M^{\rm T}$ is the transpose of matrix M and D is the diffusion matrix. From the noise correlation functions, we obtain the form of matrix D

$$\begin{aligned}D &= \mathrm{diag}[\kappa_a(2N_a+1),\kappa_a(2N_a+1),\\ &\quad\gamma_m(2N_m+1),\gamma_m(2N_m+1)].\end{aligned}\tag{12}$$

Obviously, once the CM $V(t)$ is acquired from Eq. (11), the diagonal elements $V_{ii}(t)$ ($i=1,2,3,4$) are the variances of the quadrature operators for the cavity and magnon modes. On the other hand, the degree of squeezing can also be characterized in decibel units as

$$-10\log_{10}\frac{V_{ii}(t)}{V_{\rm vac}},\tag{13}$$

where $V_{\rm vac}=0.5$ is the variance of the vacuum state.

4. Squeezed state of magnons

According to the Heisenberg uncertainty principle and the commutation relation $[X_m, Y_m] = \mathrm{i}$, as long as the variance $\langle \delta X_m^2 \rangle$ or $\langle \delta Y_m^2 \rangle$ is less than 0.5. i.e., larger than 0 dB, it can be verified that the squeezing of magnon mode is generated. To achieve squeezed state of magnons, we choose experimentally accessible parameters:[6,31,44] $\omega_a = \omega_m = 2\pi \times 10$ GHz, $\kappa_a = 2\pi \times 4$ MHz, $\gamma_m = 2\pi \times 0.4$ MHz, $g_m = 0.5\gamma_m$, $K = 10\kappa_a$, and $\Delta_a = \kappa_a$. These system parameters dynamically ensure the stability in terms of the Routh–Hurwitz criterion.[40] To clearly show the magnon squeezing, we plot time evolution of the variances $\langle \delta X_m^2 \rangle$ and $\langle \delta Y_m^2 \rangle$ in Fig. 2. From Fig. 2, we can see that the variance $\langle \delta X_m^2 \rangle$ oscillates first and then reaches the steady state quickly. Obviously, the variance $\langle \delta X_m^2 \rangle$ in the steady state reaches 2 dB and thus the squeezing of magnon mode is successfully achieved. It is well known that the basic mechanism for creating squeezing is the Hamiltonian takes the form $\delta m^2 + \delta m^{\dagger 2}$ (see Eq. (5)) so that the corresponding evolution operator is a squeezed operator. Therefore, the squeezing of magnons is successfully generated. On the other hand, according to the Heisenberg uncertain relation, the magnon mode cannot be simultaneously squeezed in the directions of X_m and Y_m. However, as shown in Fig. 2, without violating the Heisenberg's uncertain relation, via tuning the detuning Δ_m and changing the direction of magnetic field ($K_0 > 0 \to K_0 < 0$), the squeezing in terms of Y_m is also successfully generated. Therefore, either the direction of X_m or Y_m, our scheme can achieve magnon squeezing in the appropriate parameter regime.

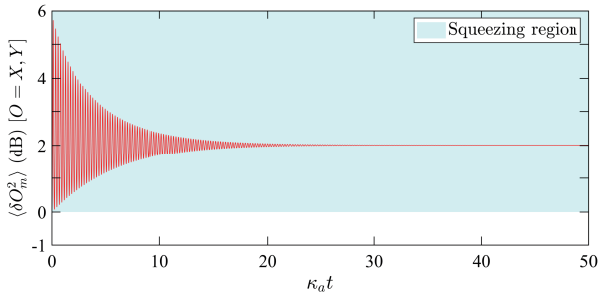


Fig. 2. Magnon variance $\langle \delta X_m^2 \rangle$ ($\langle \delta Y_m^2 \rangle$) versus time $\kappa_a t$. System parameters are $\Delta_m = -3\kappa_a$ and $\Delta_m = 3\kappa_a$ for $\langle \delta X_m^2 \rangle$ and $\langle \delta Y_m^2 \rangle$, respectively. The direction of magnetic field B_0 is along the crystallographic axis [100] and [110], respectively. See the text for other parameters.

To more intuitively present the squeezing feature in phase space, we further introduce the Wigner function to discuss the magnon squeezing. The Wigner function in terms of CM can be expressed as[45]

$$W(P) = \frac{1}{2\pi\sqrt{\mathrm{Det}[V_m]}} \exp\left[-\frac{1}{2} P^{\mathrm{T}} V_m^{-1} P\right], \tag{14}$$

where V_m is the CM of magnon mode and P refers to the two-dimensional vector $P = [X_m, Y_m]^{\mathrm{T}}$. In Fig. 3, we plot the Wigner functions of the magnon mode corresponding to initial state and steady states in Fig. 2, respectively. As shown in the left-side subplot of Fig. 3, the Wigner function neither stretches nor contracts in any axis, i.e., the magnon mode is not squeezed in either the direction of X_m nor Y_m at the beginning. However, as shown in Fig. 3(a), it is obvious that the Wigner function stretches in the vertical axis while contracts in the direction of horizontal axis. Therefore, it can be clearly found that the magnon squeezing occurs in the direction of X_m. On the other hand, when we tune $\Delta_m = 3\kappa_a$ and the magnetic field B_0 is along the crystallographic axis [110], as shown in Fig. 3(b), the Wigner function stretches along the horizontal axis while contracts along the vertical axis and the magnon squeezing is achieved in the direction of Y_m. Hence, from the point of Wigner function, it is intuitively found that, no matter in the direction of X_m or Y_m, the magnon squeezing can be successfully achieved by appropriately tuning the system parameters. This interesting feature is beneficial when the quantum fluctuation needs to be reduced in a specific direction as required in practical applications, such as quantum-enhanced measurements.[46,47]

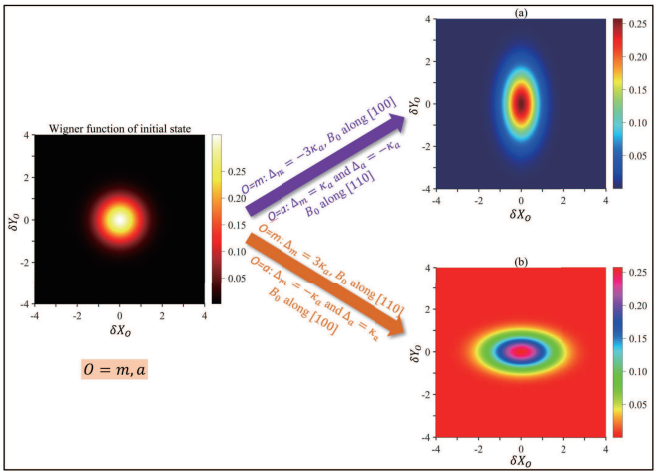


Fig. 3. Wigner functions of the magnon (cavity) mode corresponding to the initial state (left side) and steady states in Fig. 2 (right side). The system parameters are the same as those in Fig. 2.

We also plot the variances $\langle \delta X_m^2 \rangle$ and $\langle \delta Y_m^2 \rangle$ versus the detuning of magnon Δ_m and the strength of two-magnon effect K in Fig. 4 to study the influence of the Kerr nonlinearity on squeezing. As presented in Fig. 4, it is shown that the strong magnon squeezing is generated with the larger two-magnon effect strength, which is expected according to the system Hamiltonian in Eq. (5). In addition, we can also find that the detuning of magnon Δ_m and the two-magnon effect strength K have a significant influence on the stability of the system dynamics. From Fig. 4, we can easily choose the appropriate system parameters to stay away from the unstable parameter region and generate strong magnon squeezing in the desired direction.

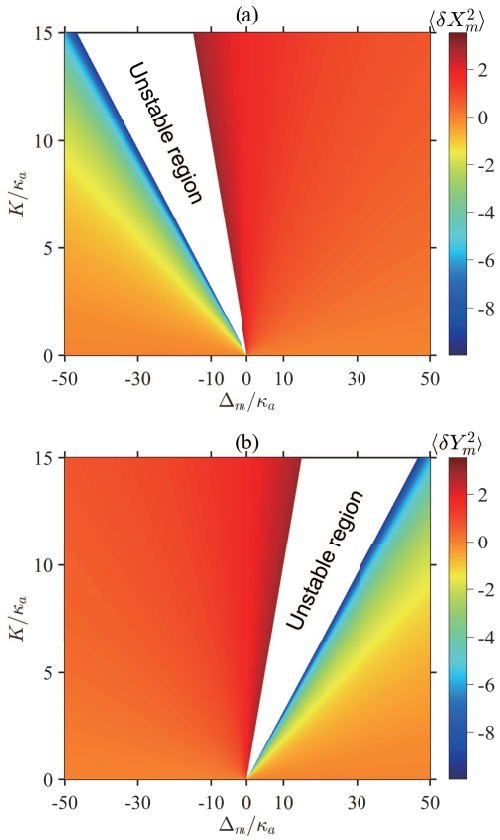


Fig. 4. Magnon variances $\langle \delta X_m^2 \rangle$ in (a) and $\langle \delta Y_m^2 \rangle$ in (b) versus the detuning of magnon Δ_m and the two-magnon effect strength K. Magnetic field B_0 is along the crystallographic axis [100] and [110] in panels (a) and (b), respectively. See the text for other parameters and the blank region denotes that the system dynamics is unstable in the corresponding parameter regime.

5. Squeezed state of photons

It is noted that the coupling term between the magnon mode and cavity mode in Eq. (5) is $g_m(\delta a \delta m^\dagger + \delta m \delta a^\dagger)$, which is the so-called cavity–magnon beam-splitter interaction and this type of interaction is generally applied to the quantum state transfer.[18,34] In the above section, we provide a detailed discussion about the generation of magnon squeezing induced by the Kerr nonlinearity. In the following, we further discuss the squeezing of cavity mode induced by the cavity–magnon beam-splitter interaction.

To show the squeezing of photons, in Fig. 5, we plot the variance dynamics of the cavity mode in different parameter regimes, respectively. From Fig. 5, it is seen that the variances $\langle \delta X_a^2 \rangle$ and $\langle \delta Y_a^2 \rangle$ both reach the steady state after the short oscillation. The steady states in the squeezing region mean that the squeezing states of photons can be successfully generated in the direction of X_a or Y_a. To show this squeezing feature more intuitively, we further plot the Wigner functions of the cavity mode in the phase space corresponding to initial state and steady states in Fig. 3. As shown of the left-side subplot in Fig. 3, the Wigner function of the initial state neither stretches nor contracts along any direction in the phase space, which corresponds to the nature that the photons at first are in a coherent state. As shown of the right-side subplots of Fig. 3, starting from the initial state, if we make use of the different parameter regimes to effectively modulate the system, the squeezing of photons will be generated in the desired direction.

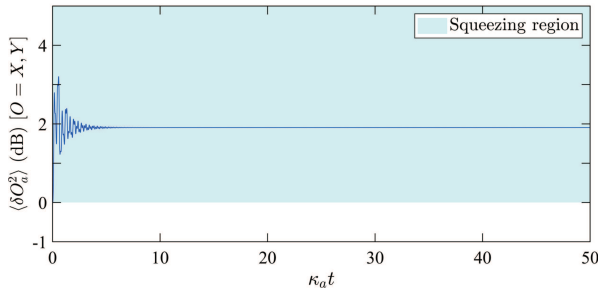


Fig. 5. Photon variance $\langle \delta X_a^2 \rangle$ ($\langle \delta Y_a^2 \rangle$) versus time $\kappa_a t$. System parameters are $\Delta_m = \kappa_a$ and $\Delta_a = -\kappa_a$ for $\langle \delta X_a^2 \rangle$ and $\Delta_m = -\kappa_a$ and $\Delta_a = \kappa_a$ for $\langle \delta Y_a^2 \rangle$, respectively. The direction of magnetic field B_0 is along the crystallographic axis [110] and [100], respectively. Here $g_m = 100\gamma_m$ and other system parameters are the same as those in Fig. 2.

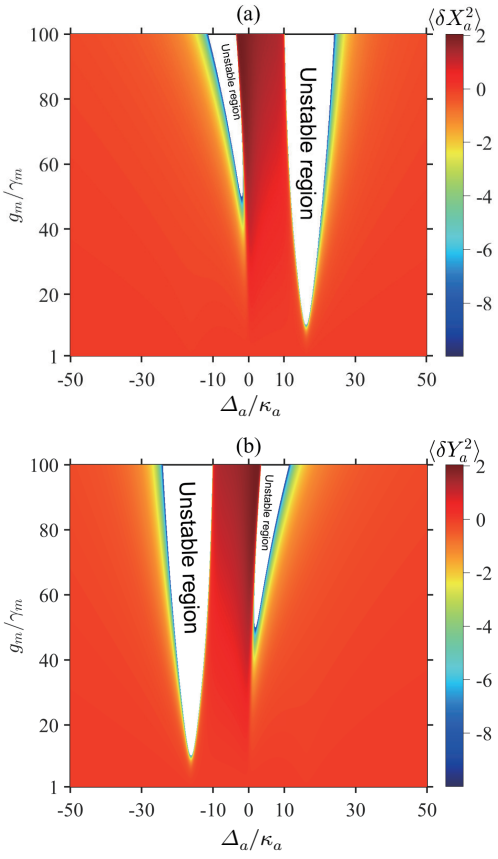


Fig. 6. Photon variances $\langle \delta X_a^2 \rangle$ in (a) and $\langle \delta Y_a^2 \rangle$ in (b) versus the cavity detuning Δ_a and the cavity–magnon coupling strength g_m. Magnetic field B_0 is along the crystallographic axis [110] and [100] in (a) and (b), respectively. The other system parameters are the same as those in Fig. 5 and the blank regions denote that the system dynamics is unstable in the corresponding parameter regime.

In addition, we also plot the variances of photon $\langle \delta X_a^2 \rangle$ and $\langle \delta Y_a^2 \rangle$ versus the cavity detuning Δ_a and the cavity–magnon coupling strength g_m in Fig. 6, respectively. As shown in Fig. 6, it is found that both the cavity detuning Δ_a and the

cavity–magnon coupling strength g_m have an obvious influence on the system stability. However, in the appropriate parameter regime, the system dynamics can keep away from the unstable region and the variance of photons in the desired direction reaches 2 dB in the steady state.

6. Experimental feasibility

In this section, we discuss the experimental feasibility of our proposed scheme. It is well known that the environment thermal noise will inevitably affect the generation of the squeezed state. To this end, the robustness of the magnon variance $\langle \delta X_m^2 \rangle$ and photon variance $\langle \delta X_a^2 \rangle$ with respect to the bath temperature T is shown in Fig. 7. From Fig. 7, it can be found that variances $\langle \delta X_m^2 \rangle$ and $\langle \delta X_a^2 \rangle$ first decrease slowly and then decrease sharply with bath temperature T. The squeezing effect persists for temperature above 300 mK, which is far larger than the experimental temperature 10 mK.[25] Hence, our scheme has strong robustness against the thermal noise. On the other hand, besides the thermal noise, another factor that affects the squeezing of photons is the cavity dissipation. In Fig. 8, we plot the photon variance $\langle \delta X_a^2 \rangle$ versus the cavity dissipation rate κ_a. It can be clearly found from Fig. 8 that the variance $\langle \delta X_a^2 \rangle$ will decrease with the increase of cavity dissipation κ_a and the squeezing of photons disappears finally. Therefore, the squeezing of photons only occurs inside the cavity.

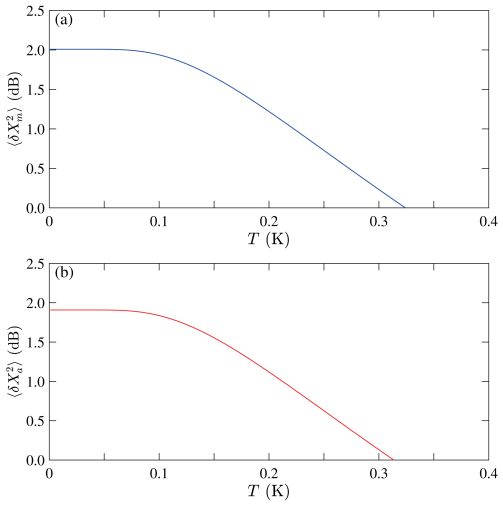


Fig. 7. Plots of the variances $\langle \delta X_m^2 \rangle$ in panel (a) and $\langle \delta X_a^2 \rangle$ in panel (b) versus the bath temperature T. The system parameters are the same as those in Figs. 2 and 5, respectively.

It should be pointed out that the cavity–magnon hybrid system with a high quality factor has been realized experimentally and the coherent coupling between magnons and microwave photons can reach the ultrastrong coupling regime.[6] On the other hand, the magnon Kerr effect has been exploited to study magnon blockade and nonreciprocal entanglement.[44] In experiment, the magnon Kerr nonlinearity can be realized via coupling the magnon mode to a superconducting qubit and the strength of Kerr effect can be tuned by adjusting the effective coupling between the magnons and qubit.[48] As an alternative method, the magnon self-Kerr nonlinearity can also be obtained via the magnetocrystalline anisotropy in YIG and the Kerr strength can be effectively tuned by changing the angle between the bias magnetic field and the crystal axis of YIG.[31] As to the detection of squeezing of magnons and photons, we can introduce an ancillary weak microwave field and by homodyning the cavity output field, the readout of the generated squeezing effect can be effectively achieved. Another detection method is to obtain the squeezing spectrum of the cavity output in the frequency domain, which carries the clear signature of squeezing effect.

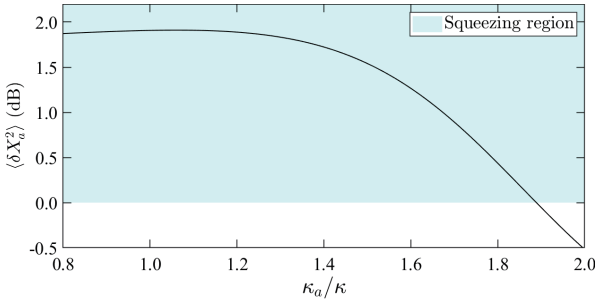


Fig. 8. Plot of the photon variance $\langle \delta X_a^2 \rangle$ versus the cavity dissipation rate κ_a. Here $T = 50$ mK and $\kappa = 2\pi \times 4$ MHz. The other system parameters are the same as those in Fig. 5, respectively.

7. Conclusion

In conclusion, we have proposed an effective scheme to generate the squeezing of magnons and photons based on the magnon Kerr effect in the cavity–magnon hybrid system. We provided a detailed discussion about the squeezing generation from the points of variance dynamics evolution and Wigner function in the phase space. We found that the squeezing of magnons can be fully generated by the magnon Kerr effect and the obtained squeezed state of magnon is stable in system dynamics. The larger squeezing of magnon could be realized by increasing the two-magnon effect strength. Meanwhile, resorting to the cavity–magnon state-swap interaction, we can further achieve the squeezing of photons. We also demonstrated that the desired squeezing direction both for magnon and photon can be successfully modulated via choosing the proper parameter regime. Our scheme provides an effective path to engineering the quantum squeezing employing the magnon Kerr effect and also has potential applications in quantum precision measurement in hybrid cavity–magnon system.

Acknowledgments

Project supported by the National Natural Science Foundation of China (Grant Nos. 12204440 and 12204292) and Fundamental Research Program of Shanxi Province, China (Grant No. 202203021212405).

References

[1] Lachance-Quirion D, Tabuchi Y, Gloppe A, Usami K and Nakamura Y 2019 *Appl. Phys. Express* **12** 070101
[2] Yuan H, Cao Y, Kamra A, Duine R A and Yan P 2022 *Phys. Rep.* **965** 1
[3] Zare Rameshti B, Viola Kusminskiy S, Haigh J A, Usami K, Lachance-Quirion D, Nakamura Y, Hu C M, Tang H X, Bauer G E and Blanter Y M 2022 *Phys. Rep.* **979** 1
[4] Zuo X, Fan Z Y, Qian H, Ding M S, Tan H, Xiong H and Li J 2024 *New J. Phys.* **26** 031201
[5] Tabuchi Y, Ishino S, Ishikawa T, Yamazaki R, Usami K and Nakamura Y 2014 *Phys. Rev. Lett.* **113** 083603
[6] Zhang X, Zou C L, Jiang L and Tang H X 2014 *Phys. Rev. Lett.* **113** 156401
[7] Zhang X, Zhu N, Zou C L and Tang H X 2016 *Phys. Rev. Lett.* **117** 123605
[8] Haigh J A, Nunnenkamp A, Ramsay A J and Ferguson A J 2016 *Phys. Rev. Lett.* **117** 133602
[9] Lachance-Quirion D, Wolski S P, Tabuchi Y, Kono S, Usami K and Nakamura Y 2020 *Science* **367** 425
[10] Xu D, Gu X K, Li H K, Weng Y C, Wang Y P, Li J, Wang H, Zhu S Y and You J Q 2023 *Phys. Rev. Lett.* **130** 193603
[11] Zhang X, Zou C L, Jiang L and Tang H X 2016 *Sci. Adv.* **2** e1501286
[12] Li J, Zhu S Y and Agarwal G S 2018 *Phys. Rev. Lett.* **121** 203601
[13] Li Y, Zhang W, Tyberkevych V, Kwok W K, Hoffmann A and Novosad V 2020 *J. Appl. Phys.* **128** 130902
[14] Li J, Wang Y P, Wu W J, Zhu S Y and You J 2021 *PRX Quantum* **2** 040344
[15] Zhang Q, Wang J, Lu T X, Huang R, Nori F and Jing H 2024 *Sci. China-Phys. Mech. Astron.* **67** 100313
[16] Clark J B, Lecocq F, Simmonds R W, Aumentado J and Teufel J D 2017 *Nature* **541** 191
[17] Peano V, Schwefel H G L, Marquardt C and Marquardt F 2015 *Phys. Rev. Lett.* **115** 243603
[18] Scully M O and Zubairy M S 1997 *Quantum Optics* (Cambridge: Cambridge University Press)
[19] Fesquet F, Kronowetter F, Renger M, Yam W K, Gandorfer S, Inomata K, Nakamura Y, Marx A, Gross R and Fedorov K G 2024 *Nat. Commun.* **15** 7544
[20] Qi S f and Jing J 2022 *Phys. Rev. A* **105** 022624
[21] Zhang G Q, Feng W, Xiong W, Su Q P and Yang C P 2023 *Phys. Rev. A* **107** 012410
[22] Qi S f and Jing J 2023 *Phys. Rev. A* **107** 013702
[23] Lu Z X, Zhu H B, Zuo X and Li J 2025 *Phys. Rev. Research* **7** 023242
[24] Liu M Y, Gong Y, Chen J, Wang Y W and Xiong W 2025 *Chin. Phys. B* **34** 057202
[25] Li J, Zhu S Y and Agarwal G S 2019 *Phys. Rev. A* **99** 021801
[26] Fan Z Y, Zhu H B, Li H T and Li J 2024 *APL Photon.* **9** 100804
[27] Zhang W, Wang D Y, Bai C H, Wang T, Zhang S and Wang H F 2021 *Opt. Express* **29** 11773
[28] Guo Q, Cheng J, Tan H and Li J 2023 *Phys. Rev. A* **108** 063703
[29] Kani A, Hatifi M and Twamley J 2025 *APL Quantum* **2** 016112
[30] Yang Z B, Jin H, Jin J W, Liu J Y, Liu H Y and Yang R C 2021 *Phys. Rev. Research* **3** 023126
[31] Wang Y P, Zhang G Q, Zhang D, Luo X Q, Xiong W, Wang S P, Li T F, Hu C M and You J Q 2016 *Phys. Rev. B* **94** 224410
[32] Wang Y P, Zhang G Q, Zhang D, Li T F, Hu C M and You J Q 2018 *Phys. Rev. Lett.* **120** 057202
[33] Zhang G, Wang Y and You J 2019 *Sci. China Phys. Mech. Astron.* **62** 987511
[34] Li J, Zhu S Y and Agarwal G S 2019 *Phys. Rev. A* **99** 021801
[35] Guo Q, Wang J X, Bai C H, Zhang Y, Li G and Zhang T 2025 *Phys. Rev. B* **112** 144422
[36] Liu Y C, Hu Y W, Wong C W and Xiao Y F 2013 *Chin. Phys. B* **22** 114213
[37] Aspelmeyer M, Kippenberg T J and Marquardt F 2014 *Rev. Mod. Phys.* **86** 1391
[38] Zhang Z, Scully M O and Agarwal G S 2019 *Phys. Rev. Research* **1** 023021
[39] Liao J Q and Law C K 2011 *Phys. Rev. A* **83** 033820
[40] DeJesus E X and Kaufman C 1987 *Phys. Rev. A* **35** 5288
[41] Vitali D, Gigan S, Ferreira A, Böhm H R, Tombesi P, Guerreiro A, Vedral V, Zeilinger A and Aspelmeyer M 2007 *Phys. Rev. Lett.* **98** 030405
[42] Mari A and Eisert J 2009 *Phys. Rev. Lett.* **103** 213603
[43] Yan D, Ren F, Huang L, Guo Y, Wang J, Gu K and Zhang H 2025 *Photonics* **12** 472
[44] Chen J, Fan X G, Xiong W, Wang D and Ye L 2023 *Phys. Rev. B* **108** 024105
[45] Weedbrook C, Pirandola S, García-Patrón R, Cerf N J, Ralph T C, Shapiro J H and Lloyd S 2012 *Rev. Mod. Phys.* **84** 621
[46] Giovannetti V, Lloyd S and Maccone L 2004 *Science* **306** 1330
[47] Li Y L, Liao C H and Xiao X 2025 *Chin. Phys. B* **34** 010307
[48] Lachance-Quirion D, Tabuchi Y, Ishino S, Noguchi A, Ishikawa T, Yamazaki R and Nakamura Y 2017 *Sci. Adv.* **3** e1603150